



ELSEVIER

Contents lists available at SciVerse ScienceDirect

Biosensors and Bioelectronics

journal homepage: [www.elsevier.com/locate/bios](http://www.elsevier.com/locate/bios)

## Rapid and sensitive detection of Nampt (PBEF/visfatin) in human serum using an ssDNA aptamer-based capacitive biosensor

Jee-Woong Park<sup>a</sup>, Sreenivasa Saravan Kallempudi<sup>b</sup>, Javed H. Niazi<sup>c,\*\*</sup>, Yasar Gurbuz<sup>b</sup>,  
Byung-Soo Youn<sup>d</sup>, Man Bock Gu<sup>a,\*</sup>

<sup>a</sup> College of Life Sciences and Biotechnology, Korea University, Anam-dong, Seongbuk-Gu, Seoul 136-713, South Korea

<sup>b</sup> Faculty of Engineering and Natural Sciences, Sabanci University, Orhanli, Tuzla, Istanbul 34956, Turkey

<sup>c</sup> Sabanci University Nanotechnology Research and Application Center, Orta Mahalle, Tuzla, Istanbul 34956, Turkey

<sup>d</sup> AdipoGen, Inc., Room 401, Venture Building B, Songdo Technopark, 7-50 Songdo-dong, Yeonsu-gu, Incheon, Korea

### ARTICLE INFO

#### Article history:

Received 3 April 2012

Received in revised form

9 May 2012

Accepted 28 May 2012

Available online 6 June 2012

#### Keywords:

Aptamer

Nampt (PBEF/visfatin)

SELEX

Capacitive biosensor

### ABSTRACT

A single-stranded DNA (ssDNA) aptamer was successfully developed to specifically bind to nicotinamide phosphoribosyl transferase (Nampt) through systematic evolution of ligands by exponential enrichment (SELEX) and successfully implemented in a gold-interdigitated (GID) capacitor-based biosensor. Surface plasmon resonance (SPR) analysis of the aptamer revealed high specificity and affinity ( $K_d=72.52$  nM). Changes in surface capacitance/charge distribution or dielectric properties in the response of the GID capacitor surface covalently coupled to the aptamers in response to changes in applied AC frequency were measured as a sensing signal based on a specific interaction between the aptamers and Nampt. The limit of detection for Nampt was 1 ng/ml with a dynamic serum detection range of up to 50 ng/ml; this range includes the clinical requirement for both normal Nampt level, which is 15.8 ng/ml, and Nampt level in type 2 diabetes mellitus (T2DM) patients, which is 31.9 ng/ml. Additionally, the binding kinetics of aptamer–Nampt interactions on the capacitor surface showed that strong binding occurred with increasing frequency (range, 700 MHz–1 GHz) and that the dissociation constant of the aptamer under the applied frequency was improved 120–240 times ( $K_d=0.3$ – $0.6$  nM) independent on frequency. This assay system is an alternative approach for clinical detection of Nampt with improved specificity and affinity.

© 2012 Elsevier B.V. All rights reserved.

### 1. Introduction

Nicotinamide phosphoribosyl transferase (Nampt) is a multifunctional protein that is also known as visfatin and pre-B cell colony-enhancing factor (PBEF). Nampt exists as the rate-limiting intracellular enzyme for nicotinamide adenine dinucleotide (NAD) synthesis beginning with nicotinamide (Revollo et al., 2007). This enzyme was also identified as cytokine PBEF, because it was shown to enhance B cell precursor maturation (Samal et al., 1994). It is also referred to as visfatin, which is an adipokine secreted by visceral adipose tissue in patients whose Nampt concentrations in serum are positively correlated with the size of visceral fat deposits (Fukuhara et al., 2005). Plasma Nampt levels are reportedly correlated with obesity and obesity-related metabolic diseases, such as type 2 diabetes mellitus (T2DM), cardiovascular diseases

(Filippatos et al., 2010), and hyperlipidemia (Chang et al., 2010) because of their association with lipoprotein and cholesterol. Moreover, Nampt was also shown to induce angiogenesis (Adya et al., 2008); hence, some studies have shown a correlation between Nampt expression and various types of cancers (Bi and Che, 2010). For example, over expression of Nampt in colorectal cancer (Nakajima et al., 2010; van Beijnum et al., 2002), prostate cancer (Wang et al., 2011), gastric cancer (Nakajima et al., 2009), and breast cancer (Kim et al., 2010) have been studied. Additionally, other diseases, such as polycystic ovary syndrome (Gen et al., 2009), chronic kidney disease (Yilmaz et al., 2008), rheumatoid arthritis (Garcia-Bermudez et al., 2011), and chronic obstructive pulmonary disease (Liu et al., 2009), were shown to be related to Nampt expression.

Many studies have examined detection of this multifunctional biomarker using the enzyme-linked immunosorbent assay (ELISA) technique (Catalan et al., 2011). However, the use of antibodies for ELISA has limitations due to stability and functional variations and discrepancies identified through clinical studies (Nusken et al., 2007). To address these limitations, we developed a Nampt-specific ssDNA aptamer through iterative rounds of

\* Corresponding author. Tel.: +82 2 3290 3417; fax: +82 2 928 6050.

\*\* Corresponding author. Tel.: +90 216 483 9879; fax: +90 216 483 9885.

E-mail addresses: [javed@sabanciuniv.edu](mailto:javed@sabanciuniv.edu) (J.H. Niazi),  
[mbgu@korea.ac.kr](mailto:mbgu@korea.ac.kr) (M.B. Gu).

selection using the FluMag-SELEX method (Stoltenburg et al., 2005). These aptamers as emerging class of affinity molecules can be chemically synthesized, easy to modify, stable, and can be used in many biosensing applications (Ellington and Szostak, 1990; Tuerk and Gold, 1990). For example, aptamers have been studied with various platforms as biological recognition elements in the development of stable biosensors, such as for a piezoelectric quartz crystal microbalance (Yao, 2009), microfluidics device (Xu, 2009), surface plasmon resonance (SPR) (Lee et al., 2008), and gold nanoparticle-based biosensor (Wang et al., 2008). Recently, label-free Faradaic impedance-based aptamer biosensors have been developed for detecting specific biomarker proteins, such as IgE (Xu et al., 2005), thrombin (Cai et al., 2006), and lysozyme (Rodriguez et al., 2005). However, since the Faradaic electrochemical system requires the addition of a redox-active species, it is not amenable to the point-of-care applications. Few studies have examined non-Faradaic techniques in which redox species are not required for signal sensing. This type of signal is often associated with changes in capacitance brought about by molecular interactions. Capacitive detection methods have been applied for many types of immunosensors, such as for bacteria detection (Laczka et al., 2008), toxin sensing (Loyprasert et al., 2010), and hormone (Liao, 2007) and protein analysis (de Vasconcelos et al., 2009b; Qureshi et al., 2010b). Recently, RNA aptamers have been employed for detecting a disease biomarker protein (C-reactive protein [CRP]) using a capacitive biosensor (Qureshi et al., 2010a). However, ssDNA aptamers have not been applied in non-Faradaic capacitive biosensors for the sensing of target proteins in serum.

In this study, Nampt-specific ssDNA aptamers were applied as recognition molecules for developing a capacitive biosensor using non-Faradaic impedance spectroscopy that converts a biological binding event into a quantifiable signal for sensitive and efficient Nampt detection. The sensor did not require the use of redox-species. For this, a capturing aptamer probe capable of binding a target was developed and immobilized on an electrode, forming an aptamer–target complex. The specific interaction of aptamer–target induced the change in dielectric properties, charge distribution, and conductivity. Regarding detecting biomarkers in serum or saliva, it is critically important in point-of-care and clinical applications. However, the sensitivity level and detection limit optimized under buffered condition are not applicable for actual samples such as serum or saliva (Rusling et al., 2010) because serum contains large numbers of different proteins that can interfere with aptamer specificity. Here, we report label-free aptamer based capacitive detection of Nampt in human serum. Our results showed that Nampt spiked in serum was successfully detected at a detection limit of 1 ng/ml, which is the most sensitive detection of Nampt in serum reported by using an aptamer. The dynamic range was found to be 1–50 ng/ml, and the immobilized aptamer on the GID capacitor showed a dissociation constant of 16.73 ng/ml (321 pM), which is much improved in comparison to the dissociation constant determined from SPR sensing platform (72.52 nM). The developed aptamer-based capacitive sensor can be used to detect Nampt in serum and has the potential for the real application in clinical diagnosis without the requirement for sample pre-treatment.

## 2. Material and methods

### 2.1. Reagents

Adipokines, including Nampt, Vaspin, and retinol binding protein 4 (RBP4), were purchased from AdipoGen (Korea). All ssDNAs were synthesized by Genotech (Korea). Bovine serum

albumin (BSA), 3-mercaptopropionic acid, N-(3-dimethylamino-propyl)-N-ethylcarbodiimide hydrochloride (EDC), and N-hydroxysuccinimide (N-hydroxy-2,5-pyrrolidinedione; NHS) were obtained from Sigma-Aldrich (Germany). All the other chemicals were of analytical grade and used without further treatment or purification. Double-distilled water (Millipore) was used in all experiments.

### 2.2. Fabrication of gold interdigitated capacitors

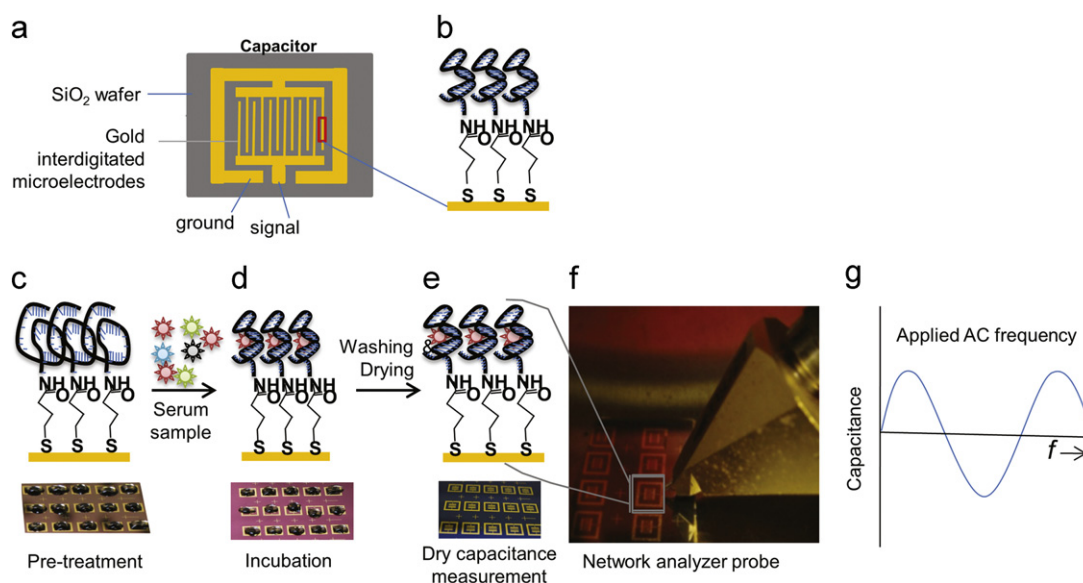
An array of gold-interdigitated (GID) electrodes was patterned on a SiO<sub>2</sub> surface using negative photolithography. A 1.8- $\mu$ m thick dual tone AZ5214E photoresist was patterned using a mask for the lift-off process. Next, a very thin titanium layer of 20 nm was deposited using direct current (DC) sputter deposition to improve the adhesion of gold onto the SiO<sub>2</sub> film. A gold layer about 180 nm thick was then deposited. The lift-off process was performed in pure acetone as the solvent. Each GID sensor array had 24 interdigitated electrode fingers with the dimension of each patterned electrode finger of  $800 \times 40 \mu\text{m}^2$  ( $l \times b$ ) with a distance between two electrode fingers of 40  $\mu$ m.

### 2.3. Immobilization of ssDNAs aptamers to capacitor electrodes

Capacitors were subjected to plasma cleaning followed by immersion in an ethanolic solution containing 100 mM of mercaptopropionic acid (MPA) overnight at room temperature for self-assembled monolayer (SAM) formation. GID electrodes were washed thoroughly using pure ethanol to remove traces of unbound MPA and dried over pure N<sub>2</sub> gas. Free carboxyl groups of MPA on the surface of GID electrodes of capacitor arrays were activated through incubation with a mixture of 200 mM of EDC and 100 mM of NHS in distilled water for 1 h. Nampt-specific aptamers (see Supporting Information [SI] Section) were then immobilized onto the surface of the GID electrode of the capacitors using covalent coupling. About 5  $\mu$ M of amine-modified aptamers were covalently coupled with activated carboxyl groups of MPA by incubating for 1 h at room temperature. The Nampt-specific amine-modified aptamer used for immobilization had the following sequence: 5'-NH<sub>2</sub>-(CH<sub>2</sub>)<sub>6</sub>-ATA CCA GCT TAT TCA ATT GGG CAG GAC AGG TGT CGG CTT GAT AG GCT GGG GTG TGT GTA GAT AGT AAG TGC AAT CT-3'. Free or unoccupied carboxyl groups were blocked by incubation with 100 mM ethanolamine for 1 h at room temperature.

### 2.4. Detection of target and counter target molecules on the capacitive biosensor

Initially, a series of Nampt concentrations of (range, 0–250 ng/ml) was prepared in binding buffer (100 mM sodium chloride, 2 mM magnesium chloride, 5 mM potassium chloride, 1 mM calcium chloride, 20 mM Tris and 0.02% Tween 20, pH 7.6). For negative controls, 50 ng/ml of 3 distinct proteins were chosen, including RBP4, Vaspin, and BSA, and prepared in binding buffer. To evaluate detection of Nampt in serum, human serum (male; blood type, AB; PANTM Biotech GmbH) was sterile-filtered using a 0.2- $\mu$ m filter disk. Various concentrations of Nampt (range, 0–250 ng/ml) were added to the serum. Similarly, 50 ng/ml each of 3 distinct non-specific and counter-target proteins (RBP4, Vaspin, and BSA), were added to the serum as negative controls. For binding assays, spiked samples were subjected to final dilution (1:5) with phosphate-buffered saline (PBS). Binding assays were performed using capacitor electrodes immobilized with aptamers against a series of target concentrations (Scheme 1). Prior to these measurements, the chips on which aptamers was immobilized had been subjected to pre-treatment of incubation at 95 °C for



**Scheme 1.** Schematic diagram of aptamer-based capacitive nicotinamide phosphoribosyl transferase (Namtpt) detection. (a) An illustration of a capacitor composed of ground and signal-interdigitated electrodes; (b) immobilized amine-functionalized aptamers on gold electrode; (c) pre-treatment of aptamer-functionalized electrodes using heat treatment and annealing under a moist chamber; (d) incubation of the sample containing target protein (serum/buffer); (e) removal of non-specific/unbound probe molecules by washing with phosphate-buffered saline (PBS) followed by drying of the capacitors, leaving only target Namtpt bound; (f) real image of network analyzer probe used to capture the signal, and (g) capacitance measurement at the scanned frequency range.

5 min followed by incubation at 4 °C for 5 min, and finally annealing at 25 °C for 15 min in a humid, airtight chamber to obtain the most stable aptamer conformation. Capacitors were then loaded with 5  $\mu$ l volume of various concentrations of target or negative control samples and incubated for 1 h.

### 2.5. Capacitance measurements

To measure dielectric parameters (impedance/capacitance), a Karl-Suss (PM-5) RF Probe Station and an Agilent-8720ES S-parameter network analyzer were used. The scanned frequency range was between 50 MHz and 1 GHz. The network analyzer was calibrated using the short-open-load-through (SOLT) method and S-parameter data of the sensor were measured. Dielectric parameters (impedance/capacitance) were measured at different stages (Scheme 1). First, dielectric parameters were measured using (a) a blank capacitor, (b) a capacitor after SAM formation with the aptamer and ethanolamine blocking, and (c) after capturing of various concentrations of target and counter-target on aptamer-immobilized capacitors. All measurements were performed in triplicate for deviation analysis. Capacitance values were exported to Matlab for analysis. Changes in capacitance or dielectric properties at an effective frequency were compared (signal from blank, control and after target capturing). Percentage relative capacitance variations were calculated based on generated data obtained within the 600–1000 MHz frequency range under standard assay conditions using the following equation:

$$\%|\Delta C| = \frac{C_{\text{target}} - C_{\text{control}}}{C_{\text{control}}} * 100$$

where  $C_{\text{target}}$  is the capacitance after binding of Namtpt target with ssDNA aptamer at a particular concentration and  $C_{\text{control}}$  is the capacitance before binding, as reported previously by de Vasconcelos et al. (2009a) for troponin T detection. Notably, the GID electrode shows both impedance and capacitive properties. Average values from 3 independent experiments and their standard deviations of dielectric measurements were plotted.

## 3. Results and discussion

### 3.1. Screening and characterization of aptamer

Namtpt-binding ssDNA aptamers were successfully selected from a random ssDNA library of  $1.2 \times 10^{14}$  variants using FluMag-SELEX (see SI Section). In all rounds of selection, 0.37 nmol of Namtpt immobilized onto the magnetic beads were incubated with the ssDNA library. After 7 rounds of SELEX, 90% of ssDNAs bound to Namtpt were recovered from the total ssDNA pool initially added, indicating saturation during the enrichment process. Counter-selection steps were introduced using counter proteins that co-exist with Namtpt in serum, such as adiponectin, RBP4, and human serum albumin (HSA), while another protein, BSA which was used for blocking of unoccupied tosyl group on the magnetic beads, was also used for counter-selection. Therefore, any ssDNAs that bound counter-targets were eliminated during the third and seventh rounds of the SELEX process (Fig. S-1). Of the 36 potential ssDNA aptamer candidates obtained using the FluMag-SELEX process, 20 ssDNA aptamers were selected based on secondary structure stability derived from minimal Gibbs free energy value ( $\Delta G$ ) calculations. Aptamers showing lower Gibbs free energy values possess high stability based on secondary structure (Table S-1). Each selected candidate was individually biotinylated and immobilized onto the streptavidin-treated gold chip for SPR analysis. Adiponectin, HSA, and RBP4 were used in the specificity test as negative controls. The aptamer no. 19 was determined to be the best candidate because it showed high specificity and a dose-dependent response (limit of detection = 25 nM) for Namtpt detection (Figs. S-2–S-4). Dose-dependent data (range, 25–400 nM) were fitted using non-linear regression analysis and the dissociation constant ( $K_d$ ) was calculated to be 72.52 nM for the no. 19 aptamer, which had a sequence of 5'-ATA CCA GCT TAT TCA ATT GGG CAG GAC AGG TGT CGG CTT GAT AG GCT GGG GTG TGT GTA GAT AGT AAG TGC AAT CT-3'. This aptamer was used for label-free Namtpt detection using GID capacitor arrays as described in Section 2. Details regarding the Namtpt aptamer screening process, its properties,

secondary structure, analysis and characterization of the selected aptamer by SPR method are all described in the SI Section.

### 3.2. Characterization of capacitor sensor surface

The sensor surface, constructed of GID capacitor electrodes on an SiO<sub>2</sub> surface and scanned using tapping mode atomic force microscopy (AFM), showed good distribution of gold particles (Fig. S-5a). An AFM 3D height map image displayed varying heights of the GID surface on the 1 × 1 μm<sup>2</sup> scanned area (Fig. S-5b). A line plot surface profile corresponding to a scanned area within 100 nm represented the height image, which clearly showed uniform heights and valleys facilitating the formation of pocketed structures on the sensor surface (Fig. S-5c). The advantage of this kind of electrode is mainly to determine the electrical responses (charge distribution/capacitance) of bimolecular interactions, such as in this case, aptamer and Nampt. Here, the capacitance change is proportional to the number of the electrodes and the area of the electrodes, while the capacitance is inversely proportional to the distance between the electrodes. Therefore, the interdigitated electrode dimension and geometry can be finely tuned that is depending upon the type of molecule to be detected (e.g., biomarkers) and its level in normal serum. The dielectric layer between the gold electrodes and their geometry eventually contributes to improving the analytical performance.

### 3.3. Detection of Nampt in buffer solution

Capacitor arrays immobilized with Nampt-specific aptamers were initially tested by incubating with various concentrations of Nampt (range, 0–250 ng/ml) in binding buffer for 1 h. The capacitive biosensor showed consistent responses in the range of 400–650 MHz; therefore, this range was selected for measuring Nampt detection in buffered condition. In this frequency range, the capacitive biosensor chip showed a specific concentration-dependent response with Nampt ranging from 1 to 50 ng/ml. Nampt concentrations greater than 50 ng/ml did not show increases likely due to saturation of binding sites of immobilized aptamers or competition between captured and free forms of the Nampt target molecule. The limit of detection of this capacitive biosensor was determined to be 1 ng/ml with a dynamic detection range of up to 50 ng/ml. This range falls within normal Nampt levels, which are 15.8 ng/ml in normal patients and 31.9 ng/ml in T2DM patients (Chen et al., 2006). For negative controls, counter targets including 50 ng/ml RBP4, Vaspin, and BSA in buffer were incubated under identical conditions using capacitors immobilized to Nampt aptamers (Fig. 1). As expected, no change in capacitance was observed with non-specific proteins on the sensor surface. These results indicate that Nampt was specifically captured on capacitors immobilized with Nampt-specific aptamers. Furthermore, our study demonstrated that sensitive detection of Nampt was achieved using Nampt-specific ssDNA aptamers, which are more stable than antibodies, within a detection range similar to the human plasma level of Nampt (Chen et al., 2006).

### 3.4. Nampt detection in human serum

Many sensors exhibit promising properties in aqueous buffer solution, but few retain their analytical properties when examined using serum samples because serum contains a large number of proteins and other biological molecules. Therefore, we tested the ability of Nampt-specific aptamers on GID capacitors to bind Nampt in complex human serum. Nampt-specific aptamers immobilized on GID capacitor arrays were incubated with various

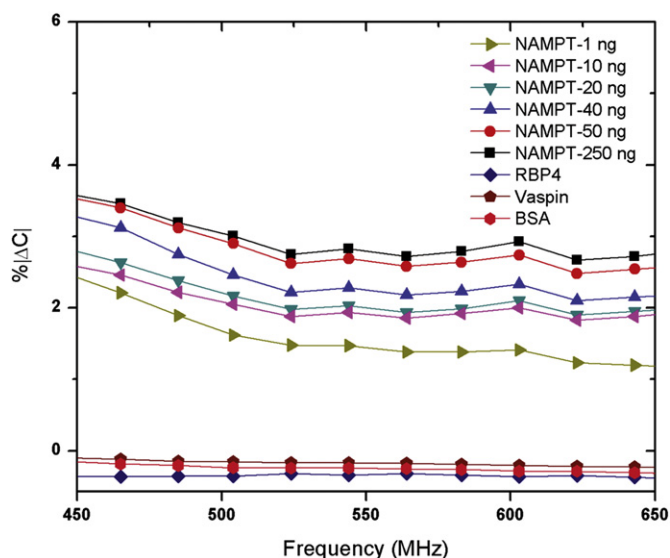


Fig. 1. Binding assays was performed for specificity tests using capacitors immobilized with nicotinamide phosphoribosyl transferase (Nampt) aptamer followed by testing with non-specific proteins (retinol binding protein 4 [RBP4], bovine serum albumin [BSA], Vaspin). A capacitance change was observed only at various concentrations of Nampt (1–250 ng/ml) in buffer condition.

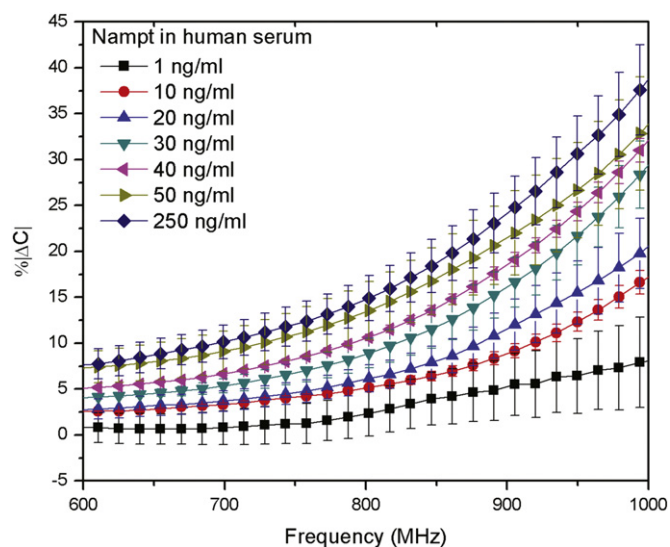


Fig. 2. Nicotinamide phosphoribosyl transferase (Nampt)-specific aptamers immobilized on gold-interdigitated (GID) capacitor arrays were incubated with various concentrations of Nampt (1–250 ng/ml) spiked in human serum, and capacitance change was recorded. A dose-dependent capacitive response to Nampt as a function of frequency was observed without false-positive signals.

concentrations of Nampt (range, 1–250 ng/ml) spiked into human serum, washed, and dried, and capacitance change was recorded. It was observed that the effective frequency range for the sensitive detection was dependent on the composition of the medium in which Nampt was present (serum/buffer). Effective frequency range for measuring Nampt in serum was found to be 600–1000 MHz, probably because of the abundant amount of interfering proteins and ions present in the serum as opposed to 450–650 MHz frequency for measuring Nampt in buffer that had no interfering molecules. We observed a dose-dependent capacitive response to Nampt as a function of frequency (Fig. 2) without any false-positive signals. Binding of Nampt-spiked serum with the Nampt-specific aptamer was achieved through the formation

of the aptamer–Nampt (ssDNA–protein) complex that is likely induced by reactions between alternatively charged side chains of amino acids in Nampt proteins and negatively charged DNA molecules (Pethig and Kell, 1987). The net charges of these complex reactions vary on the GID surface against different Nampt concentrations and therefore undergo local polarization that influences changes in dielectric properties on the sensor surface (Cole and Cole, 1941).

Additionally, particularly for the Nampt protein, the 3D structure of Nampt was made possible in the presence of nicotinamide mononucleotide (NMN) (Wang et al., 2006), which is abundant in serum, strongly indicating that NMN can stabilize the structure of recombinant Nampt. Actual serum may provide favorable conditions for efficient aptamer–target interactions, resulting in the generation of sensitive signals attributable to the physiological conditions of serum, including NMN and abundant amounts of other proteins that ensure sufficient stability of Nampt.

The detection principle of the proposed sensor is based on the change in surface capacitance as a result of charge distribution induced by the binding of target protein with ssDNA aptamers functionalized on the sensor surface. This signal is derived from the charges present on peripheral amino acids of target proteins along with negative charges of the ssDNA backbone. The bound proteins on the sensor surface tend to spin, twist, vibrate or rotate at a particular frequency. For example, the effective frequency with respect to Nampt protein in buffer was found to be in the range of 400–650 MHz (Qureshi et al., 2010a). The detection method relies on non-Faradaic current (non-redox current) induced by the formation of aptamer–protein complex on sensor surface under dry conditions as a result of change in dielectric properties, charge distribution and conductivity. The method employed in this study is label-free in nature that requires no addition of redox mediators or any reagents, rapid, easy to use and less expensive that find application in molecular interactions in native forms biomolecules (Qureshi et al., 2012). Regarding the reproducibility and the stability of the proposed biosensor, there are two possibilities by which the reproducibility and the stability of the proposed biosensor can be affected: (a) batch fabrications–microelectrode array chips are normally fabricated in clean room facility in batches. Chips fabricated in each batch have their own identity. Therefore, chips from two different batches in some occasions are not identical and, thus contribute to variations in the sensor chip responses. In this study, possible errors in reproducibility were minimized by using chips derived from a single batch. Secondly, (b) non-specific binding of co-existing molecules may affect the stability and reproducibility of the sensor response. Therefore, the GID was tested with only normal human serum that did not show significant change (one of the controls).

### 3.5. Binding kinetics of ssDNA aptamer–Nampt in serum

The change in capacitance against various concentrations of Nampt spiked in serum with a constant amount of ssDNA aptamer immobilized onto a capacitor surface was analyzed independently at four different frequencies. As a result, dose-dependent responses were observed at each frequency and capacitance responses were found to increase with increasing frequency from 700 to 1000 MHz (Fig. 3). The affinity of the aptamer for Nampt on capacitors was determined using the Langmuir adsorption isotherm and the kinetics of binding of ssDNA aptamers to its target was further supported by the characteristic responses of the bound complex at the applied frequency. Here, the large size/volume of the accumulating protein layer as a result of aptamer binding to increasing Nampt levels on the capacitor surface generally generates long relaxation

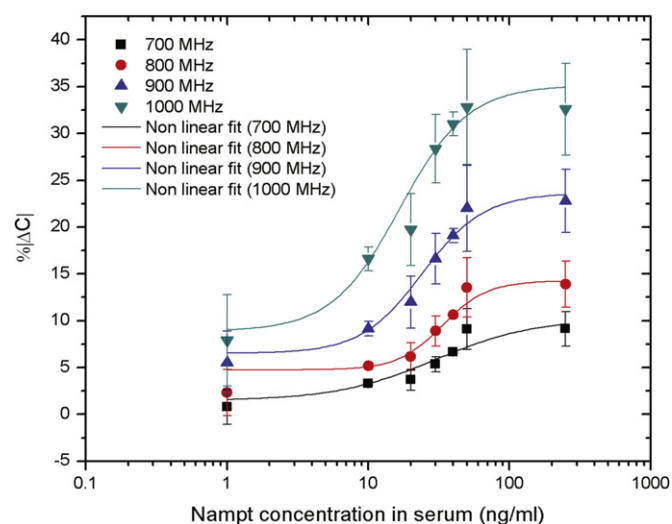


**Fig. 3.** Change in capacitance against various concentrations of nicotinamide phosphoribosyl transferase (Nampt) spiked in human serum with a constant amount of ssDNA aptamers immobilized onto the capacitor surface was analyzed independently at 4 different frequencies. Dose-dependent responses were observed at each frequency, and capacitance responses were found to increase with increasing frequency from 700 to 1000 MHz.

times that arise from rotation of the bound protein molecules, while unbound molecules were washed away. Obtained data values were fitted using non-linear regression analysis, and dissociation constants ( $K_d$ ) corresponding to analysis using an option for one-site saturation were calculated to be 29.9, 33.3, 24.1, and 16.7 ng/ml at 700, 800, 900, and 1000 MHz, respectively, which are equivalent to  $K_d$  values in the range 0.3–0.6 nM. These  $K_d$  values were well below the  $K_d$  values obtained using SPR with the same aptamer. This result indicated that stronger binding of aptamers on the sensor surface occurred at higher frequencies (900 MHz–1 GHz) and the lowest  $K_d$  value was 16.7 ng/ml (321 pM), which occurred at a frequency of 1 GHz, than that with high  $K_d$  values observed at low frequencies. Therefore, the affinity of the aptamer under the applied frequency (700 MHz–1 GHz) was improved by 120–240 times compared to that by using SPR. This is because of the angle shift in the SPR system is based on the mass of target binding on the sensor surface, as opposed to simple charge distribution in capacitive sensor. In order to enhance the response signal in SPR method, relatively large numbers of molecules are required that affect the sensitivity, affinity and the limit of detection with SPR compared with the capacitive sensor platform. Further, non-linear regression analysis of the data obtained by the interaction of varying target concentrations against capacitance change confirmed the behavior of protein molecules, including protein relaxation and surface conductance associated with movement of protein-bound ions at a particular range of frequency (Grimnes and Martinsen, 2008). Therefore, we improved the binding ability of the aptamer under an applied AC electrical frequency, which is typically not possible with other methods such as SPR.

## 4. Conclusion

In conclusion, we developed a rapid and sensitive aptamer-based Nampt detection assay in human serum. ssDNA aptamers that specifically bind Nampt were first selected using the SELEX process and characterized these potential aptamer candidates using SPR for their ability to bind Nampt. An aptamer with a  $K_d$  of 72.52 nM was applied for capacitive detection of Nampt using

GID capacitor arrays. Here, the selected aptamer was employed as a stable and reliable recognition molecule for label-free, reagentless, capacitive detection of Nampt. Nampt is a biomarker for obesity-related metabolic diseases and various types of cancers as well as some chronic diseases. Probe ssDNA aptamers were used to specifically capture Nampt protein, forming an aptamer–Nampt complex on sensor surface that induced changes in dielectric properties, surface charge distribution, and conductivity, which were measured as non-Faradaic signals. Improved affinity was observed by varying applied AC electrical frequency (range, 700–1000 MHz), which yielded low  $K_d$  values ranging from 16.7 to 33.3 ng/ml (range, 0.3–0.6 nM). The capacitive detection assay did not require additional chemicals or redox mediators for signal generation. The limit of detection was 1 ng/ml with a dynamic range of 1–50 ng/ml, which is clinically useful because normal plasma Nampt level is  $\sim$ 15 ng/ml. The aptamer-based, label-free capacitive biosensor reported in this study shows great potential for clinical diagnostic use and point-of-care applications with a sufficient detection limit.

### Acknowledgments

This work was supported by a grant from the Ministry for Health, Welfare and Family Affairs, Republic of Korea (Grant no. A081023), the National Research Foundation (NRF) of Korea grant funded by the Korea government (Ministry of Education, Science and Technology [MEST], Grant no. 2010-00579-KORANET), and the Scientific and Technological Research Council of Turkey (TUBITAK), Project no. 110E287.

### Appendix A. Supporting information

Supplementary data associated with this article can be found in the online version at <http://dx.doi.org/10.1016/j.bios.2012.05.036>.

### References

- Adya, R., Tan, B.K., Punn, A., Chen, J., Randeve, H.S., 2008. *Cardiovascular Research* 78, 356–365.
- Bi, T.Q., Che, X.M., 2010. *Cancer Biology and Therapy* 10, 119–125.
- Cai, H., Lee, T.M.H., Hsing, I.M., 2006. *Sensors and Actuators B: Chemical* 114, 433–437.
- Catalan, V., Gomez-Ambrosi, J., Rodriguez, A., Ramirez, B., Silva, C., Rotellar, F., Cienfuegos, J.A., Salvador, J., Fruhbeck, G., 2011. *Nutrition, Metabolism and Cardiovascular Diseases* 21, 245–253.
- Chang, Y.C., Chang, T.J., Lee, W.J., Chuang, L.M., 2010. *Metabolism: Clinical and Experimental* 59, 93–99.
- Chen, M.P., Chung, F.M., Chang, D.M., Tsai, J.C.R., Huang, H.F., Shin, S.J., Lee, Y.J., 2006. *Journal of Clinical Endocrinology and Metabolism* 91, 295–299.
- Cole, K., Cole, R., 1941. *Journal of Chemical Physics* 9, 341.
- de Vasconcelos, E.A., Peres, N.G., Pereira, C.O., da Silva, V.L., 2009. *Biosensors & Bioelectronics* 25, 870–876.
- de Vasconcelos, E.A., Peres, N.G., Pereira, C.O., da Silva, V.L., da Silva, E.F., Dutra, R.F., 2009. *Biosensors & Bioelectronics* 25, 870–876.
- Ellington, A.D., Szostak, J.W., 1990. *Nature* 346, 818–822.
- Filippatos, T.D., Randeve, H.S., Derdemezis, C.S., Elisaf, M.S., Mikhailidis, D.P., 2010. *Current Vascular Pharmacology* 8, 12–28.
- Fukuhara, A., Matsuda, M., Nishizawa, M., Segawa, K., Tanaka, M., Kishimoto, K., Matsuki, Y., Murakami, M., Ichisaka, T., Murakami, H., Watanabe, E., Takagi, T., Akiyoshi, M., Ohtsubo, T., Kihara, S., Yamashita, S., Makishima, M., Funahashi, T., Yamanaka, S., Hiramatsu, R., Matsuzawa, Y., Shimomura, I., 2005. *Science* 307, 426–430.
- Garcia-Bermudez, M., Gonzalez-Juanatey, C., Rodriguez-Rodriguez, L., Miranda-Filloo, J.A., Perez-Esteban, S., Vazquez-Rodriguez, T.R., Castaneda, S., Balsa, A., Fernandez-Gutierrez, B., Llorca, J., Gonzalez-Alvaro, I., Martin, J., Gonzalez-Gay, M.A., 2011. *Clinical and Experimental Rheumatology* 29, 681–688.
- Gen, R., Akbay, E., Muslu, N., Sezer, K., Cayan, F., 2009. *Gynecological Endocrinology* 25, 241–245.
- Grimnes, S., Martinsen, Ø., 2008. *Bioimpedance and Bioelectricity Basics*. Academic Press.
- Kim, J.G., Kim, E.O., Jeong, B.R., Min, Y.J., Park, J.W., Kim, E.S., Namgoong, I.S., Kim, Y.L., Lee, B.J., 2010. *Molecules and Cells* 30, 341–345.
- Laczka, O., Baldrich, E., Munoz, F.X., del Campo, F.J., 2008. *Analytical Chemistry* 80, 7239–7247.
- Lee, S.J., Youn, B.S., Park, J.W., Niazi, J.H., Kim, Y.S., Gu, M.B., 2008. *Analytical Chemistry* 80, 2867–2873.
- Liao, J.Y., 2007. *Applied Microbiology and Biotechnology* 74, 1385–1391.
- Liu, X.J., Ji, Y.L., Chen, J., Li, S.Q., Luo, F.M., 2009. *Nutrition* 25, 373–378.
- Loyprasert, S., Hedstrom, M., Thavarungkul, P., Kanatharana, P., Mattiasson, B., 2010. *Biosensors & Bioelectronics* 25, 1977–1983.
- Nakajima, T.E., Yamada, Y., Hamano, T., Furuta, K., Gotoda, T., Katai, H., Kato, K., Hamaguchi, T., Shimada, Y., 2009. *Journal of Gastroenterology* 44, 685–690.
- Nakajima, T.E., Yamada, Y., Hamano, T., Furuta, K., Matsuda, T., Fujita, S., Kato, K., Hamaguchi, T., Shimada, Y., 2010. *Cancer Science* 101, 1286–1291.
- Nusken, K.D., Nusken, E., Petrasch, M., Rauh, M., Dotsch, J., Nusken, K.D., Petrasch, M., 2007. *Clinica Chimica Acta* 382, 154–156.
- Pethig, R., Kell, D., 1987. *Physics in Medicine and Biology* 32, 933.
- Qureshi, A., Gurbuz, Y., Kallempudi, S., Niazi, J.H., 2010. *Physical Chemistry Chemical Physics* 12, 9176–9182.
- Qureshi, A., Niazi, J.H., Kallempudi, S., Gurbuz, Y., 2010. *Biosensors & Bioelectronics* 25, 2318–2323.
- Qureshi, A., Roci, I., Gurbuz, Y., Niazi, J.H., 2012. *Biosensors & Bioelectronics* 34, 165–170.
- Revollo, J.R., Grimm, A.A., Imai, S., 2007. *Current Opinion in Gastroenterology* 23, 164–170.
- Rodriguez, M.C., Kawde, A.N., Wang, J., 2005. *Chemical Communications*, 4267–4269.
- Rusling, J.F., Kumar, C.V., Gutkind, J.S., Patel, V., 2010. *Analyst* 135, 2496–2511.
- Samal, B., Sun, Y.H., Stearns, G., Xie, C.S., Suggs, S., Mccie, I., 1994. *Molecular and Cellular Biology* 14, 1431–1437.
- Stoltenburg, R., Reinemann, C., Strehlitz, B., 2005. *Analytical and Bioanalytical Chemistry* 383, 83–91.
- Tuerk, C., Gold, L., 1990. *Science* 249, 505–510.
- van Beijnum, J.R., Moerkerk, P.T.M., Gerbers, A.J., de Brune, A.P., Arends, J.W., Hoogenboom, H.R., Hufton, S.E., 2002. *International Journal of Cancer* 101, 118–127.
- Wang, B., Hasan, M.K., Alvarado, E., Yuan, H., Wu, H., Chen, W.Y., 2011. *Oncogene* 30, 907–921.
- Wang, T., Zhang, X., Bheda, P., Revollo, J.R., Imai, S., Wolberger, C., 2006. *Nature Structural and Molecular Biology* 13, 661–662.
- Wang, W.J., Chen, C.L., Qian, M.X., Zhao, X.S., 2008. *Analytical Biochemistry* 373, 213–219.
- Xu, D.K., Xu, D.W., Yu, X.B., Liu, Z.H., He, W., Ma, Z.Q., 2005. *Analytical Chemistry* 77, 5107–5113.
- Xu, Y., 2009. *Analytical Chemistry* 81, 7436–7442.
- Yao, C., 2009. *Biosensors & Bioelectronics* 24, 2499–2503.
- Yilmaz, M.I., Saglam, M., Carrero, J.J., Qureshi, A.R., Caglar, K., Eyiletlen, T., Sonmez, A., Cakir, E., Yenicesu, M., Lindholm, B., Stenvinkel, P., Axelsson, J., 2008. *Nephrology, Dialysis, Transplantation* 23, 959–965.